

Control of inflammation by stromal Hedgehog pathway activation restrains colitis

John J. Lee^{a,b,c,d,1}, Michael E. Rothenberg^{a,e,1}, E. Scott Seeley^f, Bryan Zimdahl^{a,b,c}, Sally Kawano^{a,b,c}, Wan-Jin Lu^{a,b,c}, Kunyoo Shin^{a,b,c,g}, Tomoyo Sakata-Kato^{h,2}, James K. Chen^h, Maximilian Diehn^{a,i,j}, Michael F. Clarke^{a,d,j}, and Philip A. Beachy^{a,b,c,j,3}

^aInstitute for Stem Cell Biology and Regenerative Medicine, Stanford University School of Medicine, Stanford, CA 94305; ^bDepartment of Biochemistry, Stanford University School of Medicine, Stanford, CA 94305; ^cHoward Hughes Medical Institute, Stanford University, Stanford, CA 94305; ^dDepartment of Medicine, Division of Oncology, Stanford University School of Medicine, Stanford, CA 94305; ^eDepartment of Medicine, Division of Gastroenterology and Hepatology, Stanford University School of Medicine, Stanford, CA 94305; ^fDepartment of Pathology, University of California, San Francisco, CA 94143; ^gDepartment of Life Sciences, Pohang University of Science and Technology, Pohang, Gyungbuk 37673, South Korea; ^hDepartment of Chemical and Systems Biology, Stanford University School of Medicine, Stanford, CA 94305; ⁱDepartment of Radiation Oncology, Stanford University School of Medicine, Stanford, CA 94305; and ^jStanford Cancer Institute, Stanford University School of Medicine, Stanford, CA 94305

Contributed by Philip A. Beachy, October 3, 2016 (sent for review August 18, 2016; reviewed by Terrence A. Barrett and Raymond N. DuBois)

Inflammation disrupts tissue architecture and function, thereby contributing to the pathogenesis of diverse diseases; the signals that promote or restrict tissue inflammation thus represent potential targets for therapeutic intervention. Here, we report that genetic or pharmacologic Hedgehog pathway inhibition intensifies colon inflammation (colitis) in mice. Conversely, genetic augmentation of Hedgehog response and systemic small-molecule Hedgehog pathway activation potently ameliorate colitis and restrain initiation and progression of colitis-induced adenocarcinoma. Within the colon, the Hedgehog protein signal does not act directly on the epithelium itself, but on underlying stromal cells to induce expression of IL-10, an immune-modulatory cytokine long known to suppress inflammatory intestinal damage. IL-10 function is required for the full protective effect of small-molecule Hedgehog pathway activation in colitis; this pharmacologic augmentation of Hedgehog pathway activity and stromal IL-10 expression are associated with increased presence of CD4⁺Foxp3⁺ regulatory T cells. We thus identify stromal cells as cellular coordinators of colon inflammation and suggest their pharmacologic manipulation as a potential means to treat colitis.

Hedgehog signaling | inflammatory bowel disease | colitis | interleukin-10 | colon cancer

Human inflammatory bowel disease (IBD) comprises two major disease subtypes, Crohn's disease (CD) and ulcerative colitis (UC), each associated with considerable morbidity and mortality. Genetic studies of IBD patients have uncovered loss-of-function mutations affecting IL-10 or its receptor (1, 2), but the cells and additional signaling interactions controlling inflammation remain to be fully defined. Genome-wide association studies of IBD patients have identified genes associated with CD and/or UC risk (3), as exemplified by a naturally occurring polymorphism in the coding region of the *GLII* gene, which is associated with a significant predisposition to UC in Northern Europeans (4). *GLII* encodes a transcriptional effector of Hedgehog (Hh) signaling whose genetic loss in mice causes a partial impairment of Hh response that is nonetheless compatible with development and fertility (5, 6); the increased risk of UC in association with *GLII* alteration suggests a potential involvement of Hh signaling in colon inflammation.

Results

Reduction of Hh Pathway Activity Exacerbates Acute DSS-Induced Colitis. To investigate the role of Hh signaling in IBD, we first tested whether *Gli1* inactivation increases the severity of acute dextran sulfate sodium (DSS)-induced colitis in mice (7). We obtained inconclusive results, quite distinct from those previously reported (Fig. S1) (4), possibly because of differences in housing, the genetic background, or the microbiota of the mice

used in the two studies. However, *Gli1* loss only partially impairs Hh response (5), leaving open the possibility of a more striking effect with more severe impairment.

To definitively ablate Hh signaling in the colon, we deleted the essential Hh transduction component *Smoothened* (8). Response to Hh signaling in colon is restricted to stromal cells, as indicated by the expression of *Gli1* (Fig. 1 B and C), which is not only a mediator but also a target of Hh signaling (5, 9). Stromal ablation of *Smo* (in a *Smo*^{fl/fl} background) thus can be accomplished using the stromally active *Gli1*^{CreER} driver (10) in the presence of tamoxifen to activate CreER recombinase. Indeed, tamoxifen treatment of *Gli1*^{CreER/+};*Smo*^{fl/fl} mice produced a 4.5-fold reduction in *Gli1* transcript levels by quantitative RT-PCR (qRT-PCR) analysis compared with *Gli1*^{CreER/+};*Smo*^{flox/+} control mice (Fig. S2A).

We found that, in these *Smo*-ablated mice, a light regimen of DSS exposure [2.5% (wt/vol) for 5 d, with scarcely any

Significance

Inflammatory bowel disease (IBD) is a debilitating disorder with limited treatment options. Here, we report that manipulation of Hedgehog (Hh) pathway signaling affects disease severity in the well-established dextran sulfate mouse model of colitis. Genetic and pharmacologic manipulations that decrease Hh pathway signaling in the colon worsen colitis. Conversely, manipulations that increase Hh pathway signaling ameliorate colitis. We find that Hh pathway stimulation exerts its effects partially through increased expression of the anti-inflammatory cytokine IL-10 in Hh pathway-responsive stromal cells and concomitant increases in CD4⁺Foxp3⁺ regulatory T cells in the colon. Our studies suggest that pharmacologic Hh pathway stimulation in colonic stromal cells may be a strategy to treat IBD.

Author contributions: J.J.L., M.E.R., and P.A.B. designed research; J.J.L., M.E.R., B.Z., S.K., W.-J.L., and K.S. performed research; T.S.-K. and J.K.C. contributed new reagents; J.J.L., M.E.R., E.S.S., B.Z., M.D., M.F.C., and P.A.B. analyzed data; and J.J.L. and P.A.B. wrote the paper.

Reviewers: T.A.B., University of Kentucky; and R.N.D., Medical University of South Carolina.

The authors declare no conflict of interest.

Data deposition: The microarray data reported in this paper have been deposited in the Gene Expression Omnibus (GEO) database, www.ncbi.nlm.nih.gov/geo (accession nos. GSE88990 and GSE88994).

¹J.J.L. and M.E.R. contributed equally to this work.

²Present address: Department of Immunology and Infectious Diseases, Harvard T.H. Chan School of Public Health, Boston, MA 02115.

³To whom correspondence should be addressed. Email: pbeachy@stanford.edu.

This article contains supporting information online at www.pnas.org/lookup/suppl/doi:10.1073/pnas.1616447113/-DCSupplemental.

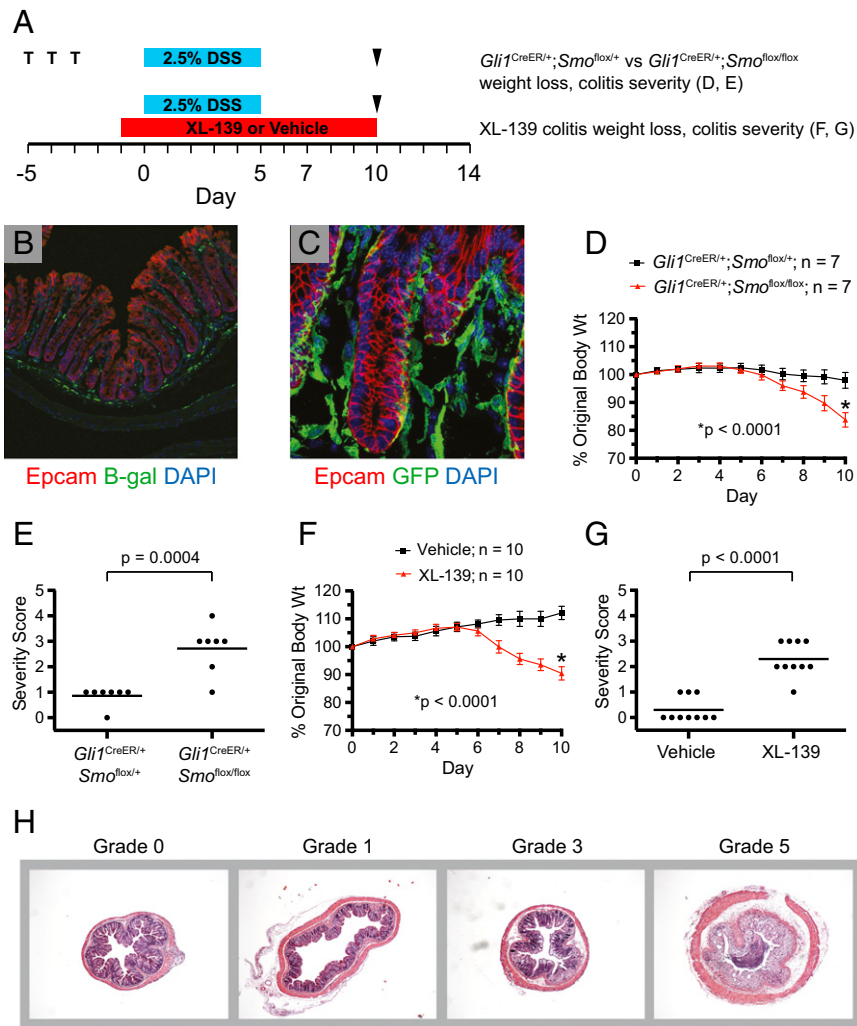


Fig. 1. Decreased Hh pathway response exacerbates acute DSS-induced colitis. (A) Overview of acute DSS-induced colitis experiments. T indicates days of tamoxifen treatment, arrowheads indicate the day of colon harvest, and colored bars indicate the duration of DSS exposure and XL-139 treatment. (B) Confocal image shows the stromal localization of *Gli1*-expressing cells using an antibody that detects nuclear expression of β -galactosidase in a *Gli1*^{LacZ/+} mouse. Epithelial cells are detected with an anti-Epcam antibody. (C) Confocal image of a colon section from a tamoxifen-treated *Gli1*^{CreER/+}; *R26*^{mTmG/+} mouse shows *Gli1*-expressing cells, as marked by expression of membrane-associated GFP, in the lamina propria closely juxtaposed to colon crypt epithelial cells (anti-Epcam antibody). (D and E) *Gli1*^{CreER/+}; *Smo*^{fl/fl} animals vs. *Gli1*^{CreER/+}; *Smo*^{fl/+} controls showed a greater loss of total body weight [(D) day 10, 83.8% vs. 97.9% original body weight, **P* < 0.0001] and more severe colitis by histologic grading [(E) 2.7 vs. 0.9, **P* = 0.0004; see H]. (F and G) XL-139-treated animals vs. vehicle-treated controls showed a greater loss of total body weight [(F) day 10, 90.5% vs. 112.1% original body weight, **P* < 0.0001] and more severe colitis [(G) day 10, 2.3 vs. 0.3 severity score, **P* < 0.0001]. (H) Representative H&E-stained cross-sections of distal colons from acute-DSS colitis experiments showing varying levels of colitis severity, as discussed in the text (Materials and Methods).

effect on wild type] sufficed to reliably induce weight loss (Fig. 1D) as well as a significant increase in the mean colitis severity score (from 0.9 to 2.7; Fig. 1E), as determined histologically by a pathologist (E.S.S.) blinded to the genetic background and treatment regimen of the mice (Fig. 1H; Materials and Methods). Complementing these genetic results, we found that pharmacologic inhibition of Hh response using the small-molecule Hh pathway antagonist XL-139 (11, 12) (Fig. S2B) also significantly accelerated weight loss (Fig. 1F) and increased the severity of colitis (from a score of 0.3 to 2.3; Fig. 1G). In summary, both genetic and pharmacologic manipulations that decisively block Hh response enhanced the development of colitis at levels of DSS exposure that scarcely produced any effect in mice with intact Hh response. The marked effect of selective *Smo* ablation by *Gli1*^{CreER} moreover shows that *Gli1*-expressing stromal cells are the critical target for colitis enhancement by Hh antagonism.

Elevated Hh Pathway Activity Decreases Acute DSS-Induced Colitis.

As reduced Hh response exacerbates acute DSS colitis, we considered the possibility that genetic or pharmacological activation of Hh signaling might ameliorate colitis. Indeed, we found that Hh signaling, although normally active at moderate levels in uninjured colon (as evidenced by expression of Hh target genes *Ptch1* and *Hhip*), is significantly suppressed during DSS-induced colitis (Fig. S3A: Vehicle–No Injury vs. Vehicle–DSS). To test whether Hh pathway activation could ameliorate colitis, we first examined colitis severity in mice with a slight general elevation of Hh activity caused by heterozygous mutation of *Ptch1* (13) (Fig. 2A), which was backcrossed over 10 generations into an FVB background to permit comparison with FVB wild-type mice. These *Ptch1*^{+/-} heterozygous mice developed significantly less severe DSS-induced colitis (severity score of 1.8 vs. 3.4; Fig. 2B) and showed decreased colitis-associated mortality (91% vs. 55% survival; Fig. 2C).

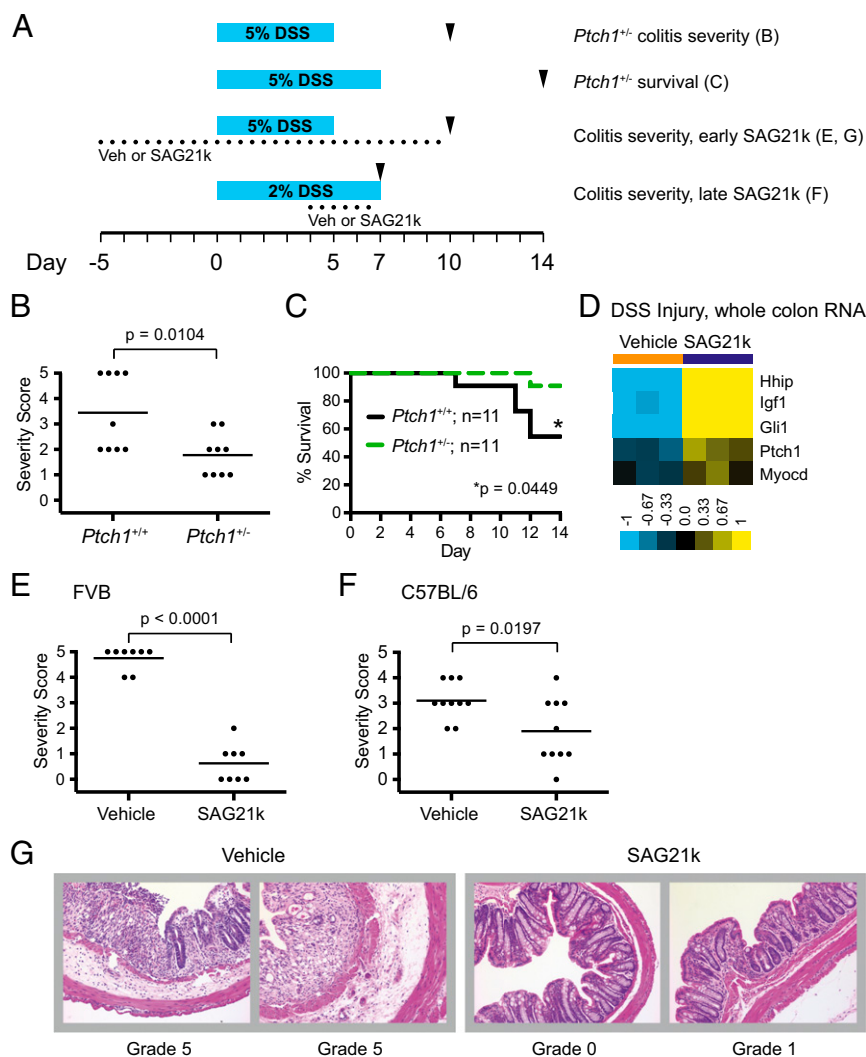


Fig. 2. Increased Hh pathway response ameliorates acute DSS-induced colitis. (A) Overview of experiments. Arrowheads indicate day of colon harvest. Colored bars indicate the duration of DSS exposure. Dots indicate the timing of either vehicle or SAG21k doses. (B) *Ptch1*^{+/-} animals show less severe colitis than *Ptch1*^{+/+} controls (average severity scores, 1.8 vs. 3.4; **P* = 0.0104). (C) Survival is increased in *Ptch1*^{+/-} vs. *Ptch1*^{+/+} animals following a 7-d period of DSS injury (90.9% vs. 54.5% survival, **P* = 0.0449, log-rank test). (D) Microarray heat map shows induction of Hh pathway targets in SAG21k (*n* = 3)- vs. vehicle (*n* = 3)-treated mice during DSS injury. Comparison of expression levels in the two treatment groups reveals the following *t* test *P* values: *Hhip*, 0.003; *Igf1*, 0.001; *Gli1*, 8.3×10^{-6} ; *Ptch1*, 0.004; and *Myocd*, 0.027. (E) SAG21k-treated FVB mice display less severe colitis than vehicle-treated FVB controls (average severity score, 0.62 vs. 4.75; **P* < 0.0001). (F) C57BL/6 mice treated with SAG21k showed less severe colitis than vehicle-treated controls by histologic grading at day 7 (average severity score, 1.9 vs. 3.1; **P* = 0.0197). SAG21k or vehicle treatment was started on day 4. (G) Representative H&E stains of distal colon show less severe colitis in SAG21k-treated mice (Right) compared with vehicle-treated mice (Left), from the experiment in E.

To further explore pathway activation, we tested the effect of a small-molecule Smoothed agonist, SAG21k (14, 15), which generates a 2.8-fold maximal elevation of *Gli1* transcript levels in the colon of uninjured FVB mice at a dose of 0.5 mg/kg twice per day (Fig. S2D). The relatively modest degree of *Gli1* induction by SAG21k in uninjured colon compared with vehicle likely is due to constitutive expression of Hh ligands in the epithelium, which generates a fairly high basal level of stromal *Gli1* expression (16–18) (Fig. 1B and C). In the setting of colitis-induced reduction of Hh pathway activity (Fig. S3A), SAG21k treatment induced a return of Hh pathway target expression to levels like those in uninjured mice treated with SAG21k (Fig. S3A: SAG21k–No Injury vs. SAG21k–DSS), thus resulting in a strong relative induction of Hh targets (e.g., a 16.0-fold change in *Gli1*, Fig. 2D; Fig. S3A).

Having established that SAG21k treatment causes a major and highly significant change in the level of Hh pathway activity in the setting of DSS-induced colitis, we examined the effects of

SAG21k treatment on colitis severity when applied either before or after the initiation of DSS injury. First, either vehicle or SAG21k was given to mice beginning 5 d before exposure to a severe colitis-inducing regimen [5% (wt/vol) DSS for 5 d; Fig. 2A]. In this setting, colitis severity was greatly reduced in the SAG21k group compared with the vehicle controls (severity score of 0.6 vs. 4.8; Fig. 2E and G). Second, mice were given either vehicle or SAG21k starting 4 d after the start of DSS treatment with a milder colitis-inducing regimen [2% (wt/vol) DSS for 7 d; Fig. 2A]. SAG21k-treated mice showed less severe colitis at day 7 compared with vehicle-treated controls (severity score of 1.9 vs. 3.1; Fig. 2F). Thus, increased Hh pathway activity, achieved genetically (in *Ptch1*^{+/-} mice) or pharmacologically (by SAG21k administration), has a strong protective effect in DSS-induced colitis. Furthermore, pharmacologic Hh pathway activation can ameliorate colitis when applied either before or after the start of DSS injury.

The Colitis-Protective Effect of Hh Pathway Activity Is Mediated in Part by Increased IL-10 Expression in *Gli1*⁺ Stromal Cells. Given that Hh pathway activation suppresses colitis, we sought to identify the cellular locus of pathway activity. Interestingly, although colitis is viewed primarily as an inflammatory disease, we found no evidence by immunofluorescence staining (Fig. S4A) or by FACS analysis (Fig. S4B) of pathway activity in hematopoietic cells of injured or uninjured colon, as indicated by absence of *Gli1* coexpression with the general hematopoietic marker, CD45; this nonoverlap of *Gli1* expression with CD45 was confirmed by nonoverlap with markers of subpopulations of hematopoietic cells (CD11b, CD11c, F4/80, or CD206, in Fig. S5 C–L). Given this absence of *Gli1* expression in hematopoietic cells of the colon, we focused directly on *Gli1*-expressing (*Gli1*⁺)

colon stromal cells to identify factors that might mediate the protective effect of Hh response. To this end, we subjected FACS-isolated *Gli1*⁺ cells from the colons of SAG21k- and vehicle-treated mice (Fig. 3A and B) to microarray analysis, and noted the expected induction by SAG21k of Hh pathway targets, including *Hhip*, *Igf1*, *Myocd*, *Gli1*, and *Ptch1* (Fig. 3C). Notably, we also observed a threefold induction in *IL-10* expression levels, confirmed as a 6.3-fold induction by qRT-PCR (Fig. 3D). In the setting of DSS-induced colitis (Fig. 3A), SAG21k induction of *IL-10* was even more dramatic in *Gli1*⁺ colon stromal cells (Fig. 3E), and this induction was not observed in FACS-isolated hematopoietic or epithelial cell populations from the colons of DSS-exposed animals (Fig. 3F; FACS plots shown in bottom two panels of Fig. S4B).

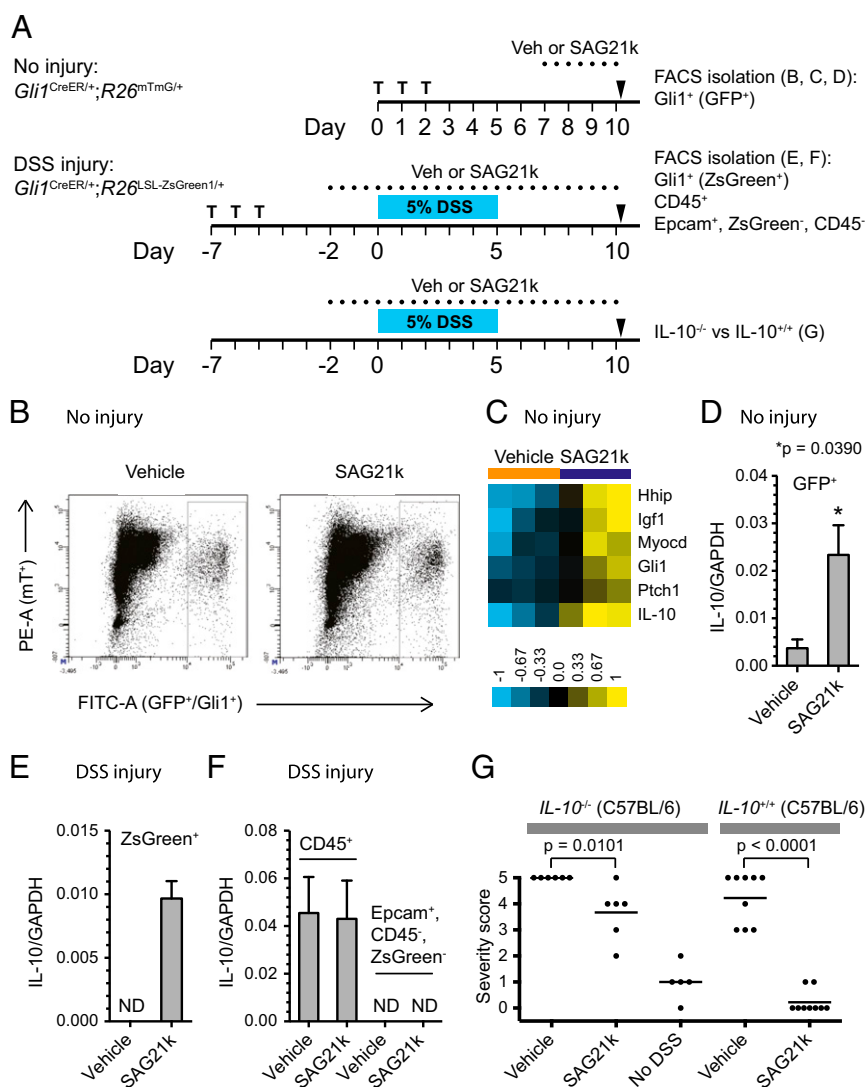


Fig. 3. The protective effect of Hh response in colitis is mediated in part by increased IL-10 expression. (A) Overview of experiments. Tamoxifen treatment (T), colon harvest (arrowheads), duration of DSS exposure (blue bars), and vehicle or SAG21k doses (dots) are shown. (B) FACS plots showing the isolation of Hh-responsive GFP⁺ marked cells (boxed, Right, in each plot) from colons of *Gli1*^{CreER/+}; *R26*^{mTmG/+} mice that were given tamoxifen, then treated with vehicle or SAG21k (as schematized in A, top diagram; *Materials and Methods*). (C) Microarray heat map shows induction of Hh pathway targets as well as *IL-10* in FACS-purified *Gli1*⁺ (GFP⁺) cells from SAG21k (n = 3)- vs. vehicle (n = 3)-treated *Gli1*^{CreER/+}; *R26*^{mTmG/+} mice. Comparison of expression levels in the two treatment groups yielded the following *t* test *P* values: *Hhip*, 0.039; *Igf1*, 0.088; *Myocd*, 0.049; *Gli1*, 0.058; *Ptch1*, 0.049; and *IL-10*, 0.009. (D) *IL-10* mRNA expression was 6.3-fold higher in FACS-purified GFP⁺ cells from noninjured mice given SAG21k vs. vehicle. (E and F) *IL-10* expression in FACS-purified cell populations from DSS-injured mice given either vehicle or SAG21k is shown. ND indicates no detection after 40 cycles of amplification. (G) The colitis-reducing effect of SAG21k was decreased in *IL-10*^{-/-} mice (1.3-unit change in mean severity score; *P* = 0.0101) compared with wild-type C57BL/6 mice (4.0-unit change; *P* < 0.0001). *IL-10*^{-/-} mice that did not receive DSS displayed a low background level of colitis (mean severity score, 1.0).

The antiinflammatory role of the IL-10 cytokine in IBD has long been known, with inactivating mutations in *IL-10* or its receptor causally linked to IBD in humans and mice (1, 2, 19–21). To determine whether *IL-10* expression indeed mediates the protective effect of Hh stromal response, we exposed *IL-10* mutant mice (*IL-10*^{-/-}) to DSS and treated with SAG21k. The *IL-10*^{-/-} strain (1), on a C57BL/6 background, is known to develop spontaneous colitis, which varies in severity depending on housing conditions: we indeed noted a low-grade colitis (average

severity score, 1.0) without DSS exposure in our colony (Fig. 3G). These *IL-10*^{-/-} mice were subjected to a 5-d exposure to 5% (wt/vol) DSS, which increased the average colitis severity score to the maximum level of 5.0 in vehicle-treated mice (Fig. 3G). This severity score was reduced to an average of 3.7 in the SAG21k treatment cohort ($P = 0.01$). The comparison vehicle-treated wild-type group, also C57BL/6, developed an average colitis severity score of 4.2 with DSS exposure, with a dramatic reduction to 0.2 upon SAG21k treatment ($P < 0.0001$). We

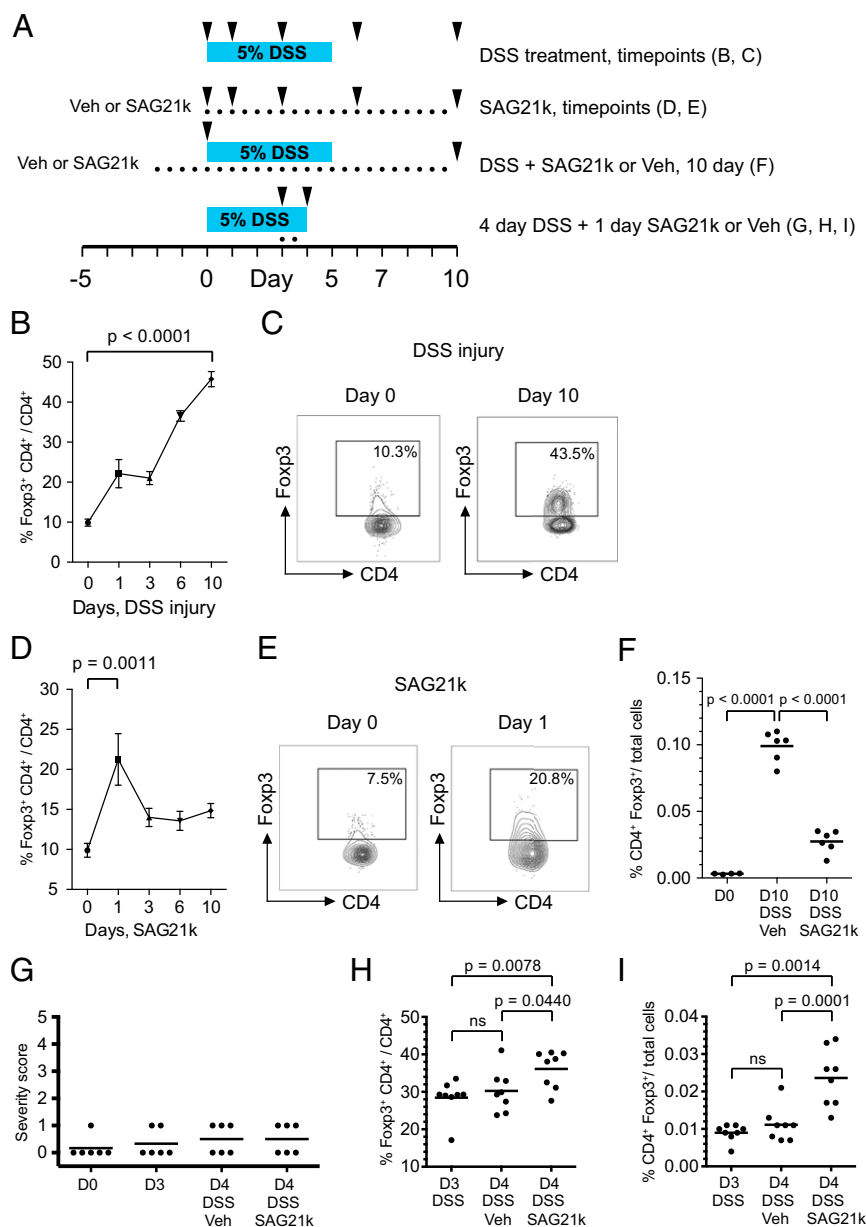


Fig. 4. Foxp3⁺ Treg levels in the colon are increased by Hh response as well as colitis. (A) Overview of experiments. Arrowheads indicate day of colon harvest. Colored bars indicate duration of DSS. Dots indicate drug doses. (B) The percentage of Foxp3⁺ cells within the CD4⁺ population increases during DSS injury [$n = 8$ mice (day 0), $n = 4$ (other time points)]. Mean percentage of Foxp3⁺/CD4⁺ cells was 9.9 on day 0 vs. 45.8 on day 10 ($P < 0.0001$). (C) Representative flow plots (gated on CD4⁺ cells) show greatly increased percentage of Foxp3⁺ cells at day 10 vs. day 0 of DSS injury. (D) Mean percentage of Foxp3⁺/CD4⁺ cells sharply increases at 1 d following SAG21k treatment (9.9, day 0, vs. 21.3, day 1; $P = 0.0011$). Afterward, Foxp3⁺ cells remain elevated through day 10 [$n = 8$ mice (day 0); $n = 4$ (other time points)]. (E) Representative flow plots show increased Foxp3⁺ cells at day 1 following SAG21k treatment compared with day 0 baseline levels. (F) After a 10-d DSS injury protocol, the percentage of CD4⁺Foxp3⁺ Treg cells increase dramatically in vehicle-treated mice. However, mice treated with SAG21k had a decreased percentage of CD4⁺Foxp3⁺ Treg cells vs. vehicle controls. (G–I) When a short course of SAG21k or vehicle was given during early DSS injury (A, bottom schema), colitis severity was minimal at all time points and there were no significant differences in treatment groups (G). In this context, SAG21k increased the percentage of CD4⁺Foxp3⁺ Tregs, both within the CD4⁺ population (H) as well as the population of total colon cells (I).

conclude from these data that, although SAG21k can partially reduce colitis in the absence of *IL-10*, induction of *IL-10* expression is required and constitutes the major mechanism by which Hh pathway activity suppresses colitis.

Hh Pathway Stimulation Increases the Amount of Foxp3⁺ Regulatory T Cells in the Colon During Early DSS Injury. *IL-10* suppresses colitis by acting to maintain expression of the transcription factor Foxp3 (22), a hallmark of regulatory T-cell (Treg) identity and function (23–25). This suggests that Hh pathway activation by SAG21k might stimulate Foxp3 expression in the setting of colitis. However, as colitis itself causes an increase in colonic Tregs (26), we were concerned that the suppression of DSS-induced colitis by SAG21k treatment might confound any SAG21k-induced augmentation of Foxp3 expression. To address this issue, we initially examined the effects of DSS and SAG21k treatments on Foxp3⁺ Treg levels independently. We first examined the

expression of Foxp3 during acute colitis and found that Foxp3 expression indeed increased in a large proportion of CD4⁺ T cells (Fig. 4A–C), with a corresponding increase in the frequency of Foxp3⁺ CD4⁺ T cells within total cells of the colon (Fig. 4F; D0 vs. D10 DSS Veh). We also found that Foxp3 expression in CD4⁺ T cells increased within 1 d of SAG21k treatment, and continued throughout our 10-d testing period (Fig. 4A, D, and E). However, when SAG21k treatment was combined with a 10-d DSS injury protocol, the population of Tregs in the colon was significantly reduced (Fig. 4F; D10 DSS Veh vs. D10 DSS SAG21k). The SAG21k treatment effect of reducing colitis severity and the accompanying reduction in Tregs thus prevails over the Treg-inducing effect of SAG21k treatment in the absence of injury.

To determine whether SAG21k could increase Treg cell levels in the setting of DSS injury independent of its effects on colitis severity, we examined the effects of SAG21k during the early

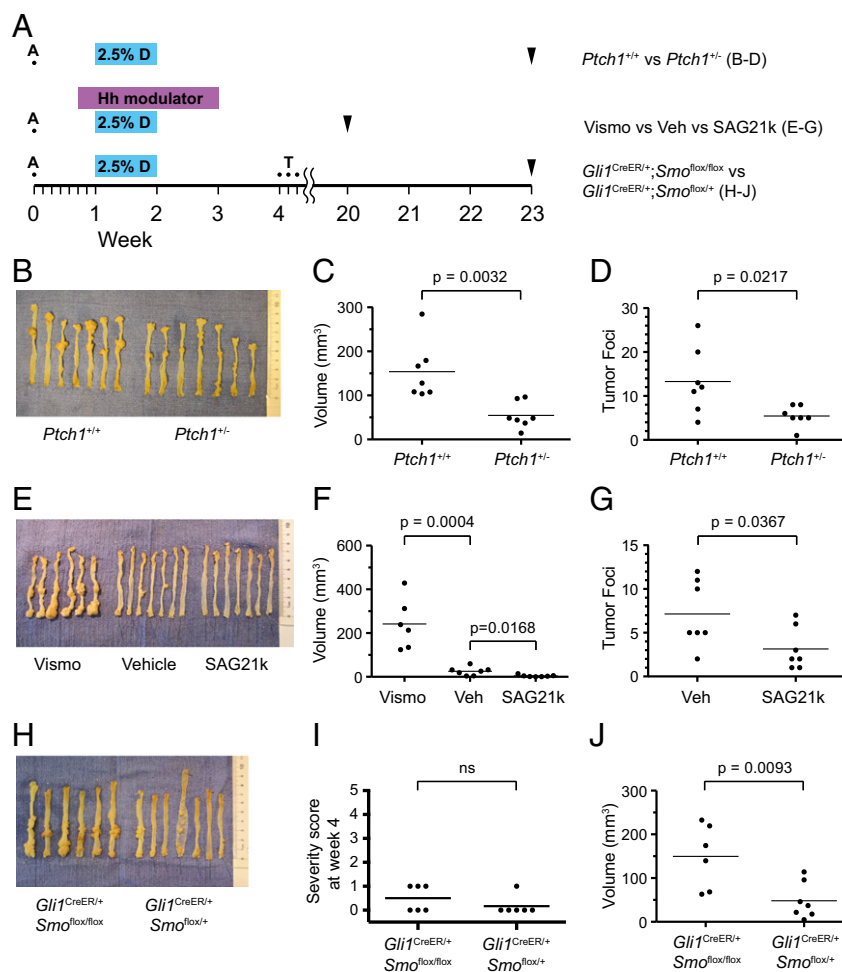


Fig. 5. Hh response reduces tumor burden in colitis-associated cancer. (A) Overview of AOM–DSS tumor induction studies. Colored bars indicate duration of exposure to DSS and Hh modulators, A denotes azoxymethane, T indicates days of tamoxifen treatment, and arrowheads indicate day of colon harvest. (B) Colons from *Ptch1^{+/+}* (n = 7) and *Ptch1^{+/-}* mice (n = 7). Distal colons are oriented toward the Top. (C) *Ptch1^{+/-}* mice develop reduced overall volume of colon tumors compared with *Ptch1^{+/+}* controls. Each data point represents the total tumor volume. (D) *Ptch1^{+/-}* mice develop fewer discrete colon tumor foci than *Ptch1^{+/+}* controls. (E) Colons from FVB mice given vismodegib (n = 6), vehicle (n = 7), or SAG21k (n = 7). Similar to XL-139, vismodegib causes a strong suppression of Hh response (Fig. S2C). Distal colons are oriented toward the Bottom. (F) The vismodegib group shows dramatically increased tumor volumes compared with vehicle (242.0 vs. 25.1 mm³, respectively; P = 0.0004), whereas the SAG21k group displays decreased tumor volumes (4.2 vs. 25.1 mm³, respectively; P = 0.0168). (G) Fewer discrete tumor foci are present in the SAG21k vs. vehicle group, whereas in the vismodegib group the tumors were too large to distinguish and count. (H) Colons from *Gli1^{CreER/+};Smo^{fl/fl}* (n = 6) and *Gli1^{CreER/+};Smo^{fl/+}* (n = 6). Distal colons are oriented toward the Bottom. (I) Two weeks after completion of DSS injury, just before administration of tamoxifen (week 4), minimal or no colitis was detected in either *Gli1^{CreER/+};Smo^{fl/fl}* or *Gli1^{CreER/+};Smo^{fl/+}* groups. There was no significant difference in mean colitis severity scores. (J) *Gli1^{CreER/+};Smo^{fl/fl}* mice develop an increased overall volume of colon tumors compared with *Gli1^{CreER/+};Smo^{fl/+}* mice (P = 0.0093).

phase of DSS injury before the onset of severe colitis and after only 1 d of SAG21k treatment. After 3 d of DSS exposure, mice were given either vehicle or SAG21k for 1 d (two doses), and Treg populations were analyzed at day 4 (Fig. 4A, bottom schema). Mice given either vehicle or SAG21k did not display differences in histologic colitis severity from each other or from day 3 control mice (Fig. 4G). However, Foxp3 expression increased in a significant proportion of CD4⁺ T cells (Fig. 4H), with a corresponding increase in the frequency of Foxp3⁺ CD4⁺ T cells within total cells of the colon (Fig. 4I). These results suggest that an early and rapid increase in Treg cells in the colon may be a mechanism by which SAG21k prevents onset or suppresses progression of colitis.

Hh Pathway Activity Reduces Tumor Burden in Colitis-Associated Colon Cancer. Given that colitis is a well-known risk factor for human colon cancer (27), we also explored the possibility that Hh pathway manipulation might also affect the extent of colitis-associated colon cancer. For our studies we used an established colitis-dependent murine cancer model [azoxymethane (AOM)–DSS] in which systemic exposure to the carcinogen AOM is followed 1 wk later by a week of exposure to DSS (28). First, we observed that genetic elevation of Hh response in *Ptch*^{+/-} mice resulted in a reduced overall tumor burden compared with *Ptch1*^{+/+} littermate controls (Fig. 5A–D). We then confirmed and extended these initial findings by pharmacologic manipulation of Hh response during the period of acute colitis in wild-type FVB mice (Fig. 5A). Pathway suppression using the small-molecule Hh antagonist vismodegib resulted in significantly greater tumor burden, whereas pathway elevation using SAG21k resulted in decreased tumor burden (Fig. 5E and F). These results are consistent with our observations that Hh pathway activity decreases colitis severity, and further suggest that decreased severity of colitis is protective against formation of colon tumors in the AOM–DSS model.

Finally, we determined whether Hh pathway manipulation outside of the period of acute colitis can influence colon tumor growth. We found that reduction of Hh response by tamoxifen-induced genetic ablation of Smo in *Gli1*^{CreER/+}; *Smo*^{fl/fl} mice, with tamoxifen administration initiated 2 wk after the end of DSS treatment and after the resolution of acute colitis, resulted in greater overall tumor burden compared with *Gli1*^{CreER/+}; *Smo*^{flox/+} controls (Fig. 5A and H–J). These results suggest that stromal Hh pathway response also reduces colon tumor growth, independent of its effects on colitis severity.

Discussion

The development of effective interventions for inflammation hinges on an understanding of its cellular coordinators. Here, we show that homeostatic suppression of inflammation in the colon is mediated by Hh-responding stromal cells. During DSS-induced colitis, Hh pathway activity is significantly reduced, and we show that pharmacologic Hh activation by SAG21k ameliorates the severity of colitis as well as progression to colitis-associated adenocarcinoma. We show that Hh activity up-regulates the expression of *IL-10* mRNA in sorted *Gli1*⁺ colonic stromal cells and that the protective effect of Hh activity is largely dependent on IL-10. Indeed, IL-10 has long been known as an anti-inflammatory cytokine and a genetic determinant of human and murine IBD (1, 2).

Previous studies have attributed the protective effect of IL-10 expression in colitis to increased expression in Treg cells of Foxp3 (22), a transcription factor required for Treg cell function (23–25). Consistent with such a protective mechanism, we noted in our DSS model that Hh pathway activation by SAG21k treatment increased the relative number of Foxp3⁺CD4⁺ Treg cells in the colon, both in a noninjured state as well as in the setting of early colitis. These previous studies identified CD11b⁺F4/80⁺

macrophages, cells of hematopoietic origin, as a major source of IL-10 that promotes Foxp3 expression (22). Our results here show that nonhematopoietic Hh-responsive stromal cells also can contribute to the IL-10-mediated protective effect and, in fact, that loss of Hh pathway response in these stromal cells renders animals significantly more vulnerable to DSS-induced colitis. We also noted a residual but significant protective effect of SAG21k in *IL-10* mutant mice, suggesting that Hh pathway activity may also protect against colitis through *IL-10*-independent mechanisms. Consistent with such a possibility, a Hh-induced antiinflammatory program of gene expression in the small intestine that did not include induction of *IL-10* was previously reported (29).

Additionally, we have demonstrated that stromal genetic or pharmacologic Hh pathway activation can reduce tumor burden in the AOM–DSS colon cancer model, as also recently reported elsewhere (30). Hence, the beneficial effects of Hh-mediated suppression of inflammation also extend to its downstream sequelae, namely progression to adenocarcinoma. Such effects of stromal Hh pathway activity have also been seen in epithelial tumor progression in the pancreas and bladder (10, 14, 31).

Finally, our work identifying a Hh-mediated program of inflammatory control has important consequences for human patients receiving systemic Hh antagonists (e.g., vismodegib) for the treatment of cancer, including locally advanced or metastatic basal cell carcinoma. In such cases, the antagonist may increase risk of IBD relapse or cause exacerbation of preexisting disease. In particular, our studies showed that Hh pathway blockade led to moderate-to-severe colitis in the presence of mild DSS exposure that alone caused little pathology (Fig. 1). Beyond exacerbation of preexisting disease, it is possible that treatment with Hh antagonists may actually increase the risk of contracting IBD. Indeed diarrhea (28% of patients) and weight loss (44% of patients) are common side effects of long-term systemic vismodegib treatment (32). Although the underlying cause of these effects was not reported, our results suggest that development of IBD certainly should be considered as a possibility. In sum, by identifying Hh-responding stromal cells as native coordinators of inflammation, our studies demonstrate the ability of a small-molecule Hh agonist to control colitis in mice, and suggest the potential application of such agents to human patients.

Materials and Methods

Mouse Strains. FVB mice were obtained from Charles River. The following strains were obtained from The Jackson Laboratory: wild-type C57BL/6 (stock no. 000664), *IL-10*^{-/-} C57BL/6 mice (1) (stock no. 002251), *R26*^{ZsGreen1/ZsGreen1} (33) (stock no. 007906), *R26*^{mTmG/mTmG} (34) (stock no. 07576), and *Smo*^{fl/fl} (35) (stock no. 04526). *Ptch*^{+/-} mice (13) were backcrossed over 10 generations to an FVB background. Other mouse strains used were as follows: *Gli1*^{CreER/CreER} (36) and *Gli1*^{lacZ/LacZ} (5). The mouse strains were intercrossed to produce the experimental cohorts. Mice were housed in a specified pathogen-free barrier facility at the Stanford School of Medicine. All experiments were conducted under Protocol 14586, approved by the Stanford Institutional Animal Care and Use Committee. For experiments in which tamoxifen-induced recombination was performed, mice were given 4 mg of tamoxifen (Sigma) per 30 g of body weight on 3 consecutive days by oral gavage. Tamoxifen was formulated as a 40 mg/mL solution in corn oil. Marking of *Gli1*⁺ cells was accomplished by tamoxifen treatment of *Gli1*^{CreER/+}; *R26*^{ZsGreen1/+} mice to activate CreER and induce ZsGreen1 expression, or by tamoxifen treatment of *Gli1*^{CreER/+}; *R26*^{mTmG/+} mice to activate CreER and induce a switch in expression of the mTmG bifluorescent reporter from mTomato to mGFP (34, 37).

DSS Colitis Studies. Solutions of DSS (MP Biomedicals; average molecular weight of 36,000–50,000) were made in sterile deionized water at the percent (weight/volume) concentrations indicated. DSS solutions were substituted for the regular drinking water at the indicated periods. All mice were between 9 and 16 wk of age at the start of each DSS injury experiment.

SAG21k was formulated as a fine suspension in PBS at a concentration of 0.05 mg/mL. SAG21k was administered to mice by i.p. injection at a dose of 0.5 mg/kg, given every 12 h. For vehicle controls, PBS was given on the same

dosing schedule. Both SAG21k and vehicle were administered in a volume of 10 μ L per g of mouse weight. The duration of the dosing is described in each figure. XL-139 was formulated in sterile deionized water at a concentration of 10 mg/mL and administered to mice by oral gavage every 72 h at a dose of 100 mg/kg. Dosing volume for XL-139 or vehicle (sterile deionized water) was 10 μ L per g of mouse weight.

Colitis severity scores were assessed in a blinded fashion by a single pathologist (E.S.S.) according to a previously described scoring system (38).

AOM-DSS Studies. AOM (Sigma) was formulated in PBS at a concentration of 1 mg/mL. Mice received a single i.p. injection of AOM at a dose of 10 mg/kg at the start of each tumor induction study, as indicated.

Vismodegib was formulated in a 10 mg/mL suspension in MCT (0.5% methylcellulose, 0.2% Tween 80). Vismodegib was given by oral gavage every 12 h at a dose of 100 mg/kg, during the time frame indicated in Fig. 5A. SAG21k was formulated and administered as described in the section above. The duration of treatment is indicated in Fig. 5A. Vehicle-treated animals received PBS injections twice daily as described above.

For tumor measurements, whole colons were dissected from killed animals. The colons were flushed internally with 10 mL of PBS with a blunt 20-gauge needle to remove feces. The colons were then cut open longitudinally and fixed in 4% paraformaldehyde/PBS [4% (wt/vol) PFA/PBS] overnight at 4 °C. To calculate the volume of each colon tumor focus, the maximal length, width, and height measurements were obtained using digital electronic calipers. Volume was calculated as an ellipsoid: $\pi/6 \times (L \times W \times H)$. The volume of each focus was summed together for the total tumor volume per colon per animal.

Immunohistochemistry. Freshly dissected colons were flushed internally with PBS with a blunt 20-gauge needle as described above. The colons were then flushed with 4% PFA/PBS to promote accelerated fixation of tissue adjacent to the lumen. Sections from the distal third of the colon were fixed overnight in 4% PFA/PBS at 4 °C. A portion of the fixed colon was submitted for paraffin embedding, sectioning, and H&E staining (Histotec) for histologic colitis severity assessment. For frozen sections, the fixed tissues were placed in 30% (wt/vol) sucrose/PBS for 12–24 h overnight at 4 °C. Afterward, the tissues were embedded into Optimal Cutting Temperature medium (Sakura Finetek).

Immunofluorescence staining was performed on 7- μ m-thick fixed-frozen colon samples. Permeabilization was performed with 0.5% Triton X-100/PBS for 15 min. Blocking was performed in 10% (vol/vol) normal goat serum (NGS)/PBS for 30 min. Primary antibody incubations were performed in 5% (vol/vol) NGS/PBS for either 2 h at room temperature or overnight at 4 °C. Secondary antibody incubations were performed in 5% (vol/vol) NGS/PBS. All washes were performed with 0.1% Tween 20/PBS (PBST). Slides were mounted with Prolong Gold with DAPI (Invitrogen).

Primary antibodies were as follows: chicken anti- β -galactosidase polyclonal (ab616; 1:1,000; Abcam); rabbit anti-GFP polyclonal (1:1,000; Novus); rat anti-mouse Epcam (clone G8.8; Developmental Studies Hybridoma Bank, University of Iowa; 1:400 of concentrated supernatant); Alexa Fluor 647 anti-mouse CD45 (clone 30F-11; 1:200; Biolegend); Alexa Fluor 647 anti-mouse CD11b (clone M170; 1:200; Biolegend); Alexa Fluor 647 anti-mouse CD11c (clone N418; 1:200; Biolegend); Alexa Fluor 647 anti-mouse F4/80 (clone BMB; 1:200; Biolegend); Alexa Fluor 647 anti-mouse CD206 (clone C068C2; 1:200; Biolegend); and rabbit anti-mouse CD31 polyclonal (ab28364; 1:100, Abcam). Secondary antibodies used for visualization were from Sigma or Jackson ImmunoResearch. Confocal microscopy was performed on Zeiss LSM 700. Images were processed with ImageJ and Adobe Photoshop CS4 software.

X-gal stains on fresh frozen colon tissue sections (10- μ m thickness) were performed as described previously (37).

FACS. Freshly dissected murine colons were gently flushed with cold calcium and magnesium-free PBS (CMF-PBS) using a blunt 20-gauge needle to remove fecal material, then cut longitudinally, and then pulse vortexed several times in CMF-PBS to remove adherent debris. The tissue was then transferred to a tissue culture dish and sliced into 1- to 2-mm³ pieces with a razor blade. Tissue fragments were subsequently washed in a 25- or 50-mL pipette by aspirating fragments in CMF-PBS up into the pipette and allowing them to settle by gravity. Tissue fragments were next digested in 10 mL of digestion buffer per colon at 37 °C in 5% (vol/vol) CO₂ and 20% (vol/vol) O₂, for 3–4 h, pipetting every 15 min. Digestion buffer consisted of advanced Dulbecco's modified Eagle medium/F12 (Invitrogen), 1 \times GlutaMax (Invitrogen), 120 μ g/mL penicillin, 100 μ g/mL streptomycin, 0.25 μ g/mL amphotericin-B, 10 mM Hepes, 10% (vol/vol) heat-inactivated FCS, with 400 U/mL Collagenase type III

(Worthington), and 100 U/mL DNase I (Worthington). The digestion was monitored under a fluorescence dissection microscope to ensure that the tissue was adequately dissociated into a single-cell suspension and that fluorescent cells, if present, were released. At this point, an equal volume of PBS plus 10 mM EDTA was added for 10 min to help disaggregate remaining clusters of cells. The cell suspension was then filtered with a 40- μ m nylon mesh filter (BD Biosciences), counted in a hemocytometer, and resuspended at $\sim 1 \times 10^6$ cells per mL in cold digestion media lacking collagenase and DNase.

Cells in staining buffer were stained in the dark on ice for 20 min with titrated fluorescently conjugated antibodies. Fluorophores varied by experiment. Antibodies included the following: Epcam–allophycocyanin–cyanine 7 or Alexa 647 or Alexa 488 (clone G8.8), CD45–phycoerythrin–Cy5 or Pacific Blue (clone 30F-11), CD4–allophycocyanin (clone RM4-5), Foxp3 (clone FJK-16s). Stainings were done with single-color controls, fluorescence-minus-one (FMO) controls, and fluorescently labeled isotype controls stained at the same antibody concentration to ensure proper compensation and gating as well as specificity of antibody binding. Intracellular staining of Foxp3 was performed using the FOXP3 Fix/Perm Buffer Set (Biolegend). After staining, cells were washed in cold CMF-PBS, pelleted, and resuspended in cold digestion media lacking collagenase, but including DNase I at 100 U/mL.

After staining, flow cytometry was immediately performed with a 100 μ m nozzle on a BD FACSAria II using FACSDiva software. Debris and doublets were excluded by sequential gating on forward-scatter area vs. side-scatter area, followed by forward-scatter width vs. forward-scatter height, followed by side-scatter height vs. side-scatter width area. Live cells were identified by exclusion of 4',6-diamidino-2-phenylindole (Molecular Probes) using FMO controls. The compensation matrix was calculated with the FACSDiva software, and was then checked manually and adjusted as necessary using single-color controls. Subpopulations within the live-cell fraction were identified and gated using isotype controls. To ensure the highest possible sorting purity, cells of interest were sorted on "single-cell" purity mode into cold digestion media lacking collagenase and DNase, and purity was then checked to ensure >95% purity. For some experiments, cells were sorted directly into TRIzol-LS (Invitrogen) to maximize RNA quality. In those cases, a test sort into cold digestion media without DNase or collagenase was performed before and after the sort into TRIzol-LS to ensure that cells sorted into TRIzol-LS were of sufficiently high purity.

Microarrays. Microarray analysis was performed by the Stanford Protein and Nucleic Acid Facility using GeneChip Mouse Genome 430 2.0 arrays (Affymetrix). For microarray experiments, RNA was reverse transcribed to cDNA with random hexamers and oligo-dT primers and T7 linkers were then added, followed by two rounds of (linear) T7-mediated amplification. RNA and cDNA quality was checked with a bioanalyzer. Microarray data were analyzed using R and Bioconductor. Raw data were normalized with the MAS5 algorithm using Custom Chip Definition Files that map to Entrez gene identifiers (Brainarray, version 19; brainarray.mbni.med.umich.edu/Brainarray/Database/CustomCDF/CDF_download.asp). Differentially expressed genes were identified using the Student t test.

qRT-PCR. To perform qRT-PCR on whole-colon samples, freshly dissected colons were first flushed with PBS using a 20-gauge blunt needle. Material from the distal third of the colon was homogenized in TRIzol Reagent (Invitrogen) using a hand-held motorized tissue homogenizer. RNA was purified using the PureLink Mini Kit (Invitrogen). The SuperScript III First-Strand Synthesis Supermix (Invitrogen) was used to prepare cDNA using random hexamers. Quantitative pPCR was performed with a Bio-Rad iCycler using the iQ SYBR Green Supermix (Bio-Rad).

To perform qRT-PCR on cell populations isolated by FACS, the RNA was purified from TRIzol-LS lysates using the PureLink Micro Kit (Invitrogen) and eluted in distilled deionized DEPC-treated RNase-free water. For experiments where more than 10,000 cells were sorted per population, the RNA was reverse transcribed with random hexamers and oligo-dT primers and then cDNA was tested directly with quantitative PCR using TaqMan assays (Invitrogen) on an ABI7900HT Thermocycler (Applied Biosystems) or designed primer pairs and SYBR Green on a Bio-Rad iCycler. Samples were loaded in triplicate on all thermal cycler runs.

For experiments where less than 10,000 cells were sorted, the RNA was reverse-transcribed and preamplified (12–20 cycles) with gene-specific primers as described (39) using the Cells-Direct kit (Invitrogen). Briefly, 1.5 μ L of RNA was added to a mixture of 5 μ L of CellsDirect 2 \times buffer, 0.1 μ L of Supersasin, 1 μ L of SuperScript III RT/Platinum Taq enzyme mix, and 2.5 μ L of a mixture of pooled primer pairs (TaqMan assays) with each assay at 0.2 \times . Reverse transcription was performed by incubating at 50 °C for 30 min, followed by preamplification with cycles of 95 °C for 2 min followed by 60 °C

for 4 min. The preamplified cDNA was then diluted 1:5 in water. qRT-PCR (40 cycles) was subsequently conducted on diluted preamplified cDNA using TaqMan assays. If there was no detection of transcript, the result was verified by two additional RT-PCR experiments. TaqMan assays used included the following: *Actb* Mm00607939_s1; *Gapdh* Mm99999915_g1; *Hprt1* Mm01545399_m1; *Gli1* Mm00494645_m1 and Mm00494654_m1; *Gli2* Mm01293116_m1; *Ptch1* Mm01306905_m1; *Hhip* Mm00469580_m1; and *IL10* Mm00439614_m1. Primers used with SYBR Green were as follows: mouse *Gli1* (forward, CCAAGCCAACCTTATGTCAGGG; reverse, AGCCCGCTCTTTGTTAA-TTTGA); mouse *Hprt1* (forward, TCAGTCAACGGGGACATAAA; reverse, GGGGTGTACTGCTTAACCAG); mouse *Ptch1* (forward, GCTACGACTATGTC-TCTCACATCAACT; reverse, GGCGACACTTTGATGAACCA); mouse *Hhip* (forward, TGAAGATGCTCTCGTTTAAGCTG; reverse, CCACCACACAGGATCTCTCC); mouse *IL-10* (forward, GCTCTTACTGACTGGCATGAG; reverse, CGCAGCTC-TAGGAGCATGTG); mouse *Ihh* (forward, GTTCACTGGTACCCTCAGATGCTCTA; reverse, GTTAGAGTCCCTCAGCTTCTGC).

Luminex Assay. Freshly dissected colons (distal third of the colon) were flushed with PBS as described above to remove feces. They were then homogenized in

RIPA buffer [10 mM Tris (pH 8.0), 140 mM NaCl, 1 mM EDTA, 0.5 mM EGTA, 1% Triton X-100, 0.1% sodium deoxycholate, 0.1% SDS] using a hand-held motorized homogenizer. The volume of RIPA buffer was >20-fold more than the volume of the sample. The RIPA buffer contained 1 tablet of cComplete Mini protease inhibitor mixture (Roche) per 10 mL of buffer. The lysate was incubated at 4 °C for 30 min, followed by centrifugation at 21,000 × g for 15 min at 4 °C. The clarified supernatant was analyzed by Luminex Assay at the Stanford Human Immune Monitoring Center.

Statistical Analyses. Graphing and statistical analyses were performed with GraphPad Prism 6 software. SE measurements are presented for all quantified data, unless otherwise specified. Group comparisons were performed with a two-tailed Student *t* test. Kaplan–Meier analyses were performed with the log-rank test.

ACKNOWLEDGMENTS. We thank Cristoph Mueller and Kyle Loh for critical reading of this manuscript, and members of the P.A.B. Laboratory for valuable input. This work was supported by the Siebel Scholar Fellowship (to J.J.L.) and the Howard Hughes Medical Institute (P.A.B.).

- Kühn R, Löhler J, Rennick D, Rajewsky K, Müller W (1993) Interleukin-10-deficient mice develop chronic enterocolitis. *Cell* 75(2):263–274.
- Spencer SD, et al. (1998) The orphan receptor CRF2-4 is an essential subunit of the interleukin 10 receptor. *J Exp Med* 187(4):571–578.
- Abraham C, Cho JH (2009) Inflammatory bowel disease. *N Engl J Med* 361(21):2066–2078.
- Lees CW, et al. (2008) Analysis of germline GLI1 variation implicates hedgehog signalling in the regulation of intestinal inflammatory pathways. *PLoS Med* 5(12):e239.
- Bai CB, Auerbach W, Lee JS, Stephen D, Joyner AL (2002) Gli2, but not Gli1, is required for initial Shh signaling and ectopic activation of the Shh pathway. *Development* 129(20):4753–4761.
- Bai CB, Joyner AL (2001) Gli1 can rescue the in vivo function of Gli2. *Development* 128(24):5161–5172.
- Laroui H, et al. (2012) Dextran sodium sulfate (DSS) induces colitis in mice by forming nano-lipocomplexes with medium-chain-length fatty acids in the colon. *PLoS One* 7(3):e32084.
- Varjosalo M, Taipale J (2007) Hedgehog signaling. *J Cell Sci* 120(Pt 1):3–6.
- Bai CB, Stephen D, Joyner AL (2004) All mouse ventral spinal cord patterning by hedgehog is Gli dependent and involves an activator function of Gli3. *Dev Cell* 6(1):103–115.
- Shin K, et al. (2014) Hedgehog signaling restrains bladder cancer progression by eliciting stromal production of urothelial differentiation factors. *Cancer Cell* 26(4):521–533.
- Low JA, de Sauvage FJ (2010) Clinical experience with Hedgehog pathway inhibitors. *J Clin Oncol* 28(36):5321–5326.
- Zaidi AH, et al. (2013) Smoothed inhibition leads to decreased proliferation and induces apoptosis in esophageal adenocarcinoma cells. *Cancer Invest* 31(7):480–489.
- Goodrich LV, Milenković L, Higgins KM, Scott MP (1997) Altered neural cell fates and medulloblastoma in mouse patched mutants. *Science* 277(5329):1109–1113.
- Lee JJ, et al. (2014) Stromal response to Hedgehog signaling restrains pancreatic cancer progression. *Proc Natl Acad Sci USA* 111(30):E3091–E3100.
- Brunton SA, et al. (2009) Potent agonists of the Hedgehog signaling pathway. *Bioorg Med Chem Lett* 19(15):4308–4311.
- Kosinski C, et al. (2010) Indian hedgehog regulates intestinal stem cell fate through epithelial-mesenchymal interactions during development. *Gastroenterology* 139(3):893–903.
- van Dop WA, et al. (2009) Depletion of the colonic epithelial precursor cell compartment upon conditional activation of the hedgehog pathway. *Gastroenterology* 136(7):2195–2203.
- van Dop WA, et al. (2010) Loss of Indian Hedgehog activates multiple aspects of a wound healing response in the mouse intestine. *Gastroenterology* 139(5):1665–1676.
- Engelhardt KR, Grimbacher B (2014) IL-10 in humans: Lessons from the gut, IL-10/IL-10 receptor deficiencies, and IL-10 polymorphisms. *Curr Top Microbiol Immunol* 380:1–18.
- Pils MC, et al. (2010) Monocytes/macrophages and/or neutrophils are the target of IL-10 in the LPS endotoxemia model. *Eur J Immunol* 40(2):443–448.
- Glocker EO, et al. (2009) Inflammatory bowel disease and mutations affecting the interleukin-10 receptor. *N Engl J Med* 361(21):2033–2045.
- Murai M, et al. (2009) Interleukin 10 acts on regulatory T cells to maintain expression of the transcription factor Foxp3 and suppressive function in mice with colitis. *Nat Immunol* 10(11):1178–1184.
- Fontenot JD, Gavin MA, Rudensky AY (2003) Foxp3 programs the development and function of CD4⁺CD25⁺ regulatory T cells. *Nat Immunol* 4(4):330–336.
- Wan YY, Flavell RA (2007) Regulatory T-cell functions are subverted and converted owing to attenuated Foxp3 expression. *Nature* 445(7129):766–770.
- Williams LM, Rudensky AY (2007) Maintenance of the Foxp3-dependent developmental program in mature regulatory T cells requires continued expression of Foxp3. *Nat Immunol* 8(3):277–284.
- Wang L, et al. (2015) T regulatory cells and B cells cooperate to form a regulatory loop that maintains gut homeostasis and suppresses dextran sulfate sodium-induced colitis. *Mucosal Immunol* 8(6):1297–1312.
- Farraye FA, Odze RD, Eaden J, Itzkowitz SH (2010) AGA technical review on the diagnosis and management of colorectal neoplasia in inflammatory bowel disease. *Gastroenterology* 138(2):746–774.
- Tanaka T, et al. (2003) A novel inflammation-related mouse colon carcinogenesis model induced by azoxymethane and dextran sodium sulfate. *Cancer Sci* 94(11):965–973.
- Zacharias WJ, et al. (2010) Hedgehog is an anti-inflammatory epithelial signal for the intestinal lamina propria. *Gastroenterology* 138(7):2368–2377.
- Gerling M, et al. (2016) Stromal Hedgehog signalling is downregulated in colon cancer and its restoration restrains tumour growth. *Nat Commun* 7:12321.
- Rhim AD, et al. (2014) Stromal elements act to restrain, rather than support, pancreatic ductal adenocarcinoma. *Cancer Cell* 25(6):735–747.
- Basset-Seguín N, et al. (2015) Vismodegib in patients with advanced basal cell carcinoma (STEVE): A pre-planned interim analysis of an international, open-label trial. *Lancet Oncol* 16(6):729–736.
- Madisen L, et al. (2010) A robust and high-throughput Cre reporting and characterization system for the whole mouse brain. *Nat Neurosci* 13(1):133–140.
- Muzumdar MD, Tasic B, Miyamichi K, Li L, Luo L (2007) A global double-fluorescent Cre reporter mouse. *Genesis* 45(9):593–605.
- Long F, Zhang XM, Karp S, Yang Y, McMahon AP (2001) Genetic manipulation of hedgehog signaling in the endochondral skeleton reveals a direct role in the regulation of chondrocyte proliferation. *Development* 128(24):5099–5108.
- Ahn S, Joyner AL (2004) Dynamic changes in the response of cells to positive hedgehog signaling during mouse limb patterning. *Cell* 118(4):505–516.
- Shin K, et al. (2011) Hedgehog/Wnt feedback supports regenerative proliferation of epithelial stem cells in bladder. *Nature* 472(7341):110–114.
- Geboes K, et al. (2000) A reproducible grading scale for histological assessment of inflammation in ulcerative colitis. *Gut* 47(3):404–409.
- Rothenberg ME, et al. (2012) Identification of a cKit⁺ colonic crypt base secretory cell that supports Lgr5⁺ stem cells in mice. *Gastroenterology* 142(5):1195–1205.